

# Euglycemic Hyperinsulinemic Clamp and Oral Glucose Load in Stimulating Myocardial Glucose Utilization During Positron Emission Tomography

M. Juhani Knuuti, Pirjo Nuutila, Ulla Ruotsalainen, Markku Saraste, Risto Härkönen, Aapo Ahonen, Mika Teräs, Merja Haaparanta, Uno Wegelius, Arto Haapanen, Jaakko Hartiala, and Liisa-Maria Voipio-Pulkki

*Departments of Clinical Physiology, Medicine, Radiology and Turku Medical PET Research Center, University of Turku, Turku, Finland*

To enable assessment of myocardial viability, myocardial glucose utilization has commonly been stimulated by oral glucose loading. To compare the effects of glucose loading and insulin and glucose infusion (insulin clamp) on PET fluorodeoxyglucose ( $[^{18}\text{F}]\text{FDG}$ ) myocardial scan image quality and regional myocardial glucose utilization rate (rMGU), eight patients with angiographically documented coronary artery disease and previous myocardial Q-wave infarction were studied twice, once during insulin clamp and once 1 hr after oral glucose loading. The rMGU rates were derived by graphic Patlak analysis in 33 normal, 10 scar and 6 "hot spot" myocardial segments. Infusion of insulin and glucose gave stable plasma-glucose and serum-insulin levels during imaging. In contrast, glucose loading caused marked changes in plasma-glucose and insulin concentrations. The image quality was clearly superior and the fractional utilization rates of  $[^{18}\text{F}]\text{FDG}$  were twice as high during insulin clamp than after glucose loading ( $p < 0.0001$ ). Due to the higher plasma-glucose levels after glucose loading, the calculated rMGU in normal, scar and hot spot myocardial segments was comparable between the two protocols. The insulin clamp technique makes it possible to adjust and maintain a metabolic steady state during the PET study. It does not alter  $[^{18}\text{F}]\text{FDG}$  uptake patterns in different myocardial areas when compared to the standard glucose loading protocol, but this technique results in superior image quality and permits the use of smaller  $[^{18}\text{F}]\text{FDG}$  patient doses.

**J Nucl Med 1992; 33:1255-1262**

**P**ositron emission tomography (PET) imaging of the heart with  $[^{18}\text{F}]\text{-2-fluoro-2-deoxy-D-glucose}$  ( $[^{18}\text{F}]\text{FDG}$ ) has emerged as a clinically feasible method to assess myo-

cardial viability in patients with myocardial infarction (1-4). However, analysis of the myocardial images has remained largely qualitative. The recent development of a relatively simple method to derive regional myocardial glucose utilization rates (rMGU) from  $[^{18}\text{F}]\text{FDG}$  PET data (5) has made it possible to measure rMGU noninvasively in humans. The deoxyglucose model of Sokoloff et al. (6, 7) and Patlak graphical analysis (8) assume that the metabolic conditions such as plasma-glucose and rMGU remain constant during data acquisition. Because the myocardial uptake of  $[^{18}\text{F}]\text{FDG}$  depends on several metabolic variables (9), attempts have been made to standardize the metabolic environment by performing the studies either when the patient has fasted, after glucose has been administered or postprandially, depending on the issue to be resolved (1-4). Fasting improves the detection of increased  $[^{18}\text{F}]\text{FDG}$  utilization caused by ischemia. However, Gropler et al. (10) have recently showed significant heterogeneity in rMGU in fasting subjects, which limits the specificity of detecting myocardial ischemia by  $[^{18}\text{F}]\text{FDG}$  studies in fasting patients. After glucose loading, on the other hand, the myocardial uptake of  $[^{18}\text{F}]$  radioactivity was more homogeneously distributed. Oral glucose loading (50 g) has been commonly used before injection of  $[^{18}\text{F}]\text{FDG}$  to stimulate rMGU when areas of decreased perfusion or wall motion have been scrutinized for viability by PET (2, 4).

Oral administration of glucose does not produce a metabolic steady-state (11) and therefore the application of quantitative analysis to these studies is problematic. The euglycemic hyperinsulinemic clamp technique is a method that mimics the postabsorptive steady-state (12) and has emerged as an alternative to oral glucose loading in stimulating rMGU (13-17). However, there is only limited information available on the effect of this procedure on myocardial uptake of  $[^{18}\text{F}]\text{FDG}$ . We have investigated the outcome of myocardial  $[^{18}\text{F}]\text{FDG}$  PET studies under eu-

Received Sept. 18, 1991; revision accepted Jan. 31, 1992.

For reprints contact: Dr. Juhani Knuuti, Department of Clinical Physiology, Turku University Central Hospital, SF-20520 Turku, Finland.

**TABLE 1**  
Summary of Clinical Data

Patient No.	Age	Infarction		Angiography		EF
		No.	Location	No. of sten. vessels	Location of significant stenoses ( $\geq 50\%$ )	
1	20	1	ANT	1	LAD	80
2	55	3	INF	3	LCA, LAD, LCX, RCA	30
3	58	1	ANT	3	LAD, RCA, LCX	58
4	54	1	ANT	1	LAD	64
5	49	1	ANT	2	LAD, LCX	55
6	47	1	ANT	1	LAD	59
7	61	1	POST	3	LCA, LAD, LCX, RCA	77
8	43	2	INF	2	LAD, RCA	67

ANT = anterior; EF = ejection fraction % in angiocardiology; INF = inferior; LAD = left anterior descending coronary artery; LCA = left main coronary artery; LCX = left circumflex coronary artery; POST = posterior; and RCA = right coronary artery.

glycemic hyperinsulinemia clamp in patients with coronary artery disease and compared the results to glucose loading.

## METHODS

### Subjects

Eight nondiabetic male patients (age  $48 \pm 2$  yr, mean  $\pm$  s.e.) with angiographically confirmed stable coronary artery disease and a previous Q-wave infarction participated in the study (Table 1). The myocardial infarctions had been verified electrocardiographically and fulfilled the enzymatic criteria (creatinase kinase  $2190 \pm 430$  IU/liter, normal  $<270$  IU/liter). The mean interval between the infarction and the PET study was 19 mo (range 4–36 mo). No patient had clinical signs of heart failure and left ventricular ejection fractions averaged  $61\% \pm 14\%$  as determined by angiocardiology.

To localize normal, infarcted and possibly ischemic areas, all patients underwent coronary angiography, angiocardiology, SPECT exercise-rest perfusion imaging and two-dimensional echocardiography. The SPECT studies and angiographies were performed within 3 mo of the PET study (mean time interval  $1.1 \pm 1.3$  mo). Echocardiography was performed on the day of the first PET study. Each subject gave written informed consent. The study protocol was approved by the ethical committee of the Turku University Central Hospital.

### Study Design

Two PET studies in each patient were performed in random order within 2 wk. All antianginal medication except nitrates was withdrawn at least 24 hr prior to the PET studies. All studies were performed after a 12-hr overnight fast. Two catheters were inserted, one in an antecubital vein for infusion of glucose and insulin and injection of [ $^{18}\text{F}$ ]FDG, and another in a vein of contralateral hand that was warmed ( $70^\circ\text{C}$ ) for sampling of arterialized venous blood. Both studies consisted of a 60-min preinjection period and a 60-min imaging period. In the load study, the patients ingested 50 g glucose at the beginning of the study. In the clamp study, insulin and glucose infusions were started and plasma-glucose was stabilized during the preinjection period. Fluorine-18-FDG was injected and dynamic imaging was performed for 60 min.

At the beginning of the clamp study, serum insulin was raised by a primed, continuous infusion of insulin (12). The rate of

insulin infusion was 1 mU/kg/min. During hyperinsulinemia, normoglycemia was maintained with 20% glucose infused at an appropriate rate. The rate of the glucose infusion was adjusted according to plasma-glucose determinations, which were performed every 10 min from arterialized venous blood. Blood samples were taken at 30-min intervals for determination of serum insulin concentrations. In the load study, glucose and insulin infusions were replaced with saline infusion. Heart rate and systolic blood pressure were monitored during the study to calculate the double product.

### Measurement of rMGU

*Preparation of [ $^{18}\text{F}$ ]FDG.* This was synthesized with an automatic apparatus by a modified method of Hamacher et al. (18). The [ $^{18}\text{F}$ ]-F- had a specific activity of 150 Ci/ $\mu\text{mol}$  (19,20); radiochemical purity exceeded 99%.

*Image Acquisition.* The patients were positioned supine in an eight-ring ECAT 931/08-12 tomograph (CTI Corp, Knoxville, TN) with a measured axial resolution of 6.7 mm and a 6.5 mm in plane. To correct for photon attenuation, transmission imaging was performed for 30 min prior to emission scanning with a removable ring source containing  $^{68}\text{Ge}$  (total counts  $15\text{--}30 \times 10^6$  per plane).

At 60 min after starting the insulin clamp or after glucose loading, 6.6–8.4 mCi (240–310 MBq) of [ $^{18}\text{F}$ ]FDG were injected intravenously over 30 sec (mean dose  $7.7 \pm 0.1$  mCi in the load studies and  $7.8 \pm 0.1$  mCi in the clamp studies). Dynamic imaging was started simultaneously and continued for 60 min ( $8 \times 15$  sec,  $2 \times 30$  sec,  $2 \times 120$  sec,  $1 \times 180$  sec,  $4 \times 300$  sec,  $3 \times 600$  sec). Twenty-five blood samples were taken for measurement of radioactivity in plasma.

*Image Processing and Corrections.* All data were corrected for deadtime, decay and photon attenuation and reconstructed in a  $256 \times 256$  matrix. The final in-plane resolution in reconstructed and Hann-filtered images was 8 mm FWHM. Thirty-five to 40 elliptical regions of interest (ROIs) were placed on six representative transaxial ventricular slices in each patient, avoiding myocardial borders, and time-activity curves were calculated. The myocardial time-activity curves were corrected for partial volume using information from two-dimensional echocardiographic measurements of wall thickness and left ventricular diameter and phantom studies (21,22). Plasma time-activity curves were generated from the calibrated arterialized venous blood samples

by a nonlinear least-squares fitting routine; this information yielded the tracer input curve.

**Calculation of rGU.** Plasma and tissue time-activity curves were analyzed graphically (8). The slope of the plot in graphic analysis is equal to the utilization constant of [ $^{18}\text{F}$ ]FDG,  $K_i$ , which represents the fractional rate of tracer transport and phosphorylation. In this study, the last six time points were used to determine the slope by linear regression.

The myocardium was divided into eight segments: anterobasilar, anterior, anteroseptal, lateral, inferoseptal, apical, inferior and posterobasilar. The segmental division was the same as used by Brunken et al. (2,23), with the exception that the large inferior segment was divided into two parts. The mean  $K_i$  for each segment was used for further calculations. The rate of myocardial glucose uptake in each segment is given by  $K_i \times P_{\text{gluc}}/\text{LC}$ , where LC (lumped constant) is used to correct for differences in the transport and metabolism of [ $^{18}\text{F}$ ]FDG and glucose (24–26). In this study, the LC in the myocardium was assumed to be 0.67 (24).

### Coronary Angiography

All patients underwent selective coronary angiography by standard techniques. A 50% or greater diameter reduction in a major epicardial branch was considered significant. A two-view angiocardiography was also performed to obtain and localize wall motion abnormalities. The results were scored segmentally into four groups: (1) normal, (2) hypokinetic, (3) akinetic and (4) dyskinetic. The cine tapes were blindly analyzed by two experienced radiologists. Discordances were resolved by consensus.

### Exercise SPECT Perfusion Imaging

For SPECT perfusion studies of the myocardium, either  $^{201}\text{Tl}$  (four patients) or  $^{99\text{m}}\text{Tc-MIBI}$  (methoxy-isobutyl-isonitrile) was used. Both studies consisted of imaging immediately after exercise and at rest and used two tracer injections ( $\text{Tl}$ , 2 mCi + 1 mCi,  $\text{MIBI}$  5 mCi + 20 mCi). A Siemens-Rota SPECT gamma camera (Siemens Gammasonics, Des Moines, IL) was used for SPECT. The tomographic images of the heart were reconstructed in 10-mm thick transaxial slices and three perpendicular planes. The radioactivity in the eight anatomic segments was assessed qualitatively and blindly by two experienced nuclear medicine specialists. The results from the stress and rest images were scored according to the following scale: (1) normal, (2) clear but modest defect, (3) notable defect and (4) complete defect. A defect was considered reversible if it disappeared (normal result in rest images), partially reversible if its score decreased by  $\geq 1$  or fixed if there was no change between the exercise and rest images. There was one instance of discordance, which was resolved by consensus.

### Two-Dimensional Echocardiography

Two-dimensional echocardiography (Aloka SSD 870, Aloka Inc., Japan) was performed according to the semiquantitative method recommended by the American Society of Echocardiography Committee on Standards (27), but the segmental subdivision was modified to correspond to the PET studies. The segmental left ventricular wall motion and thickening was scored according to the following scale: (1) normal, (2) hypokinetic, (3) akinetic and (4) dyskinetic. In addition, the abnormal wall segments were considered to be thinned if the wall thickness was reduced by  $\geq 25\%$  compared with the adjacent normal segments.

### Alignment of Myocardial Segments with Different Methods

For the purpose of this study, echocardiography, angiocardiography and SPECT results were used to classify different myocardial segments as normal, scar or potentially ischemic as precisely as possible. The SPECT and PET transaxial slices were visually aligned and compared to each other and the results of the transaxial images were assigned to the eight segments with the help of a heart map phantom designed for this study. The wall motion abnormalities in angiography and echocardiography were also localized in the segmental heart map phantom. All results were first localized by the physician, who performed each study. The segmental scores from each method were finally aligned and pooled together by the first author. To avoid errors induced by misalignment, only segments with concordant results by all modalities were classified as normal or scar tissue as explained later in the results.

### Analytical Procedures

Plasma-glucose was determined in duplicate by the glucose oxidase method (28) using a Beckman Glucose Analyzer II (Beckman Instruments, CA). Plasma-free insulin was measured by radioimmunoassay (29).

### Statistical Analysis

Independent samples were compared by analysis of variance. Paired samples were compared by paired comparisons t-test. All results are expressed as mean values and standard error of mean (s.e.m.).

## RESULTS

### Metabolic Characteristics During Insulin Clamp and After Glucose Loading

Insulin clamping gave stable plasma-glucose and insulin levels throughout the time of imaging (glucose  $5.1 \pm 0.2$  mmol/liter and insulin  $104 \pm 7$  mU/liter, Figs. 1 and 2). In contrast to this, after glucose loading plasma-glucose concentrations increased from normoglycemia to  $10.2 \pm 0.4$  mmol/l and then declined to  $8.4 \pm 0.8$  mmol/l by 60 min of injection. Correspondingly, the mean plasma-insulin concentrations increased from  $13 \pm 2$  to  $65 \pm 10$  mU/liter and then declined to  $45 \pm 8$  mU/liter. There was

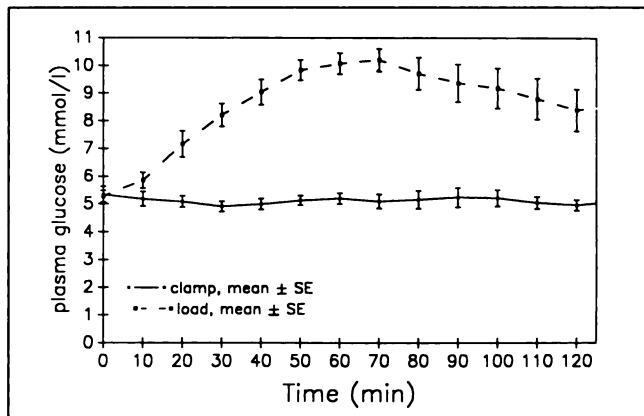


**FIGURE 1.** Mean plasma-glucose levels after glucose loading and during insulin clamp.

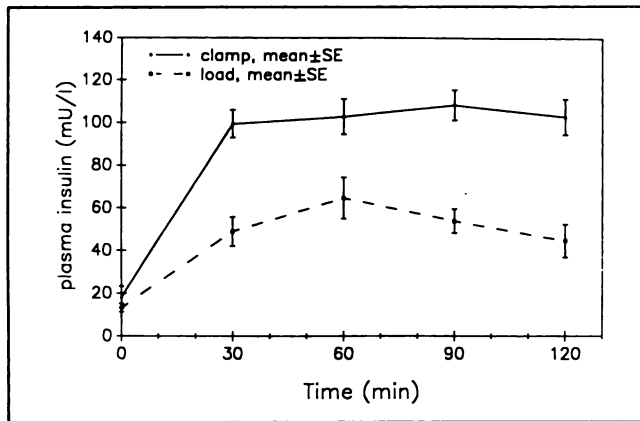


**FIGURE 2.** Mean plasma-insulin levels after glucose loading and during insulin clamp.

no difference in the double product during the two PET studies ( $7600 \pm 240$  during the clamp,  $7140 \pm 340$  after glucose loading, ns).

#### Echocardiography, Angiocardiology and SPECT

As explained above, echocardiography, angiocardiology and SPECT results were used to classify the eight myocardial segments in each patient as normal, scar or potentially ischemic. To avoid errors induced by misalignment, only segments with concordant results by all modalities were classified as normal or scar tissue. The criteria for normal segments at rest were: normal result (score 1) in exercise and rest SPECT perfusion study, score 1 in echocardiography and angiocardiology and  $<75\%$  stenosis in the corresponding coronary artery. The criteria for myocardial scar were: wall motion score  $>3$  in angiocardiology and echocardiography with thinned myocardium and a fixed defect (score  $\leq 3$ ) by SPECT.

By definition, 64 myocardial segments were identified in 8 patients. The number of normal segments was 33. Ten segments were scarred. At least three normal segments and one scar segment were identified in each patient. The remaining 21 segments represented various combinations of abnormalities in the three modalities and were considered to be viable, yet potentially ischemic (see below).

#### Qualitative Analysis of PET Images

The visually observed image quality was superior in the clamp studies in comparison to images obtained after glucose loading (Figs. 3 and 4). Image quality was also excellent during insulin clamp in the three patients with impaired glucose tolerance after glucose loading. There were no obvious differences in the size or intensity of the defects or hot spots between the clamp and glucose load studies.

The visual appearance of the last 10-min PET image was compared with the results of segment classification by other modalities. All normal segments showed homogeneous accumulation of [ $^{18}\text{F}$ ]FDG. All segments classified as scar had lower [ $^{18}\text{F}$ ]FDG activity than normal segments, but the intensity of the defect varied. In 8 of the 10 scar segments, there was  $\geq 50\%$  reduction of radioactivity compared with the normal segments in each patient. In the remaining two segments, the reduction was milder (30%–50%).

Among the 21 segments classified as abnormal but viable, 6 segments gave the visual impression of hot spots. These six segments (in three patients) were associated with critical coronary stenoses (90%–100%). Five of these six segments also demonstrated reversible SPECT perfusion defects. This group was analyzed separately and considered to represent chronic ischemia or postischemically increased glucose utilization (30).

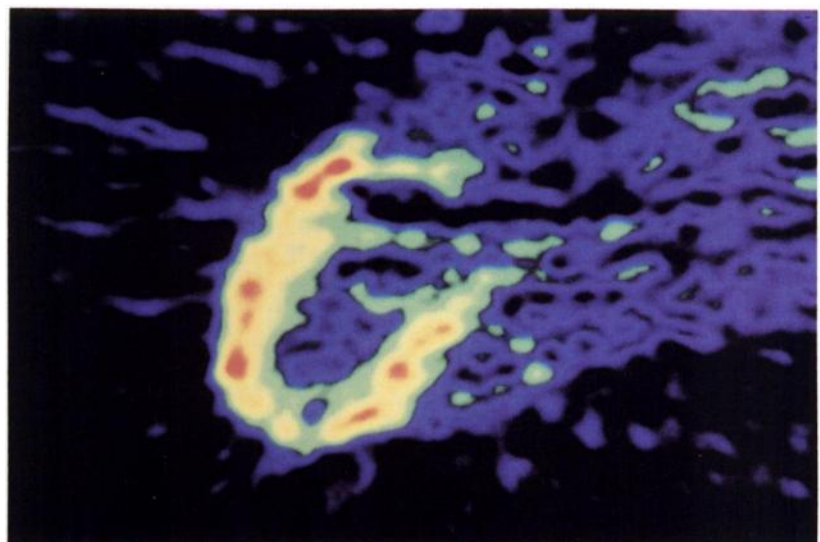


**FIGURE 3.** An example of a transaxial image obtained after glucose loading (Patient 6, 50 min after [ $^{18}\text{F}$ ]FDG injection).

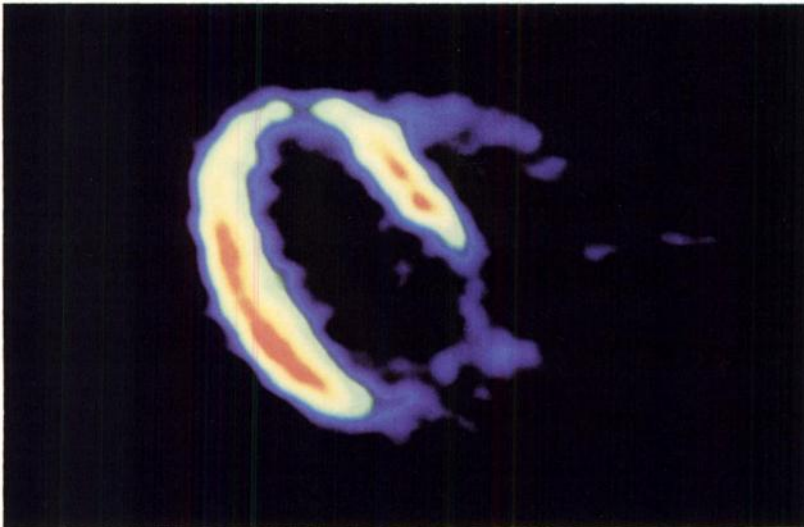


**FIGURE 4.** An example of transaxial image obtained during insulin clamp. (Patient 6, 50 min after  $[^{18}\text{F}]\text{FDG}$  injection, the same level as in Fig. 3).

### Quantitative Analysis of PET Studies

At the end of the study, the radioactivity in the normal myocardial segments was  $1.01 \pm 0.08 \mu\text{Ci/ml}$  during clamp and  $0.79 \pm 0.06 \mu\text{Ci/ml}$  after glucose loading ( $p = 0.028$ , clamp/load 128%) (Fig. 5). The mean plasma radioactivity was  $0.059 \pm 0.008 \mu\text{Ci/ml}$  and  $0.16 \pm 0.02$ , respectively ( $p = 0.0001$ ) (clamp/load 37%). The mean ratio of radioactivity in normal myocardium and plasma was higher during insulin clamp than after glucose loading ( $18.9 \pm 2.3$  versus  $5.4 \pm 0.8$ ,  $p = 0.0001$ ).

Figure 6 shows an example of different  $K_i$  values obtained by graphical analysis of  $[^{18}\text{F}]\text{FDG}$  uptake after glucose loading and during clamp in a normal segment in Patient 6. For the 49 segments included in the final analysis, the mean fractional utilization ( $K_i$ ) of  $[^{18}\text{F}]\text{FDG}$  after glucose loading was  $53\% \pm 2\%$  of the values obtained during insulin clamp ( $52\%$  in 33 normal segments,  $54\%$

in 10 scar segments and  $51\%$  in 6 hot spot segments) (Fig. 7). Due to the higher plasma-glucose levels after glucose loading, the rMGU results were similar in all segment groups during both protocols (Fig. 8). The mean rMGU in normal segments was  $68.6 \pm 3.1 \mu\text{mol}/100\text{g}/\text{min}$  after glucose loading and  $73.7 \pm 2.9 \mu\text{mol}/100\text{g}/\text{min}$  during clamp (ns). In scar and hot spot segments, the corresponding rMGU values were  $37.4 \pm 4.5$  and  $90.3 \pm 2.0 \mu\text{mol}/100\text{g}/\text{min}$  after glucose loading and  $38.8 \pm 5.2$  and  $96.6 \pm 5.1 \mu\text{mol}/100\text{g}/\text{min}$  during clamp (ns between load and clamp studies).

To study the variability of the rMGU within and between the subjects in the normal segments, the standard deviations (s.d.) of the rMGU values after glucose loading were compared with the values during clamp. There was no difference in the variation of rMGU between the pa-

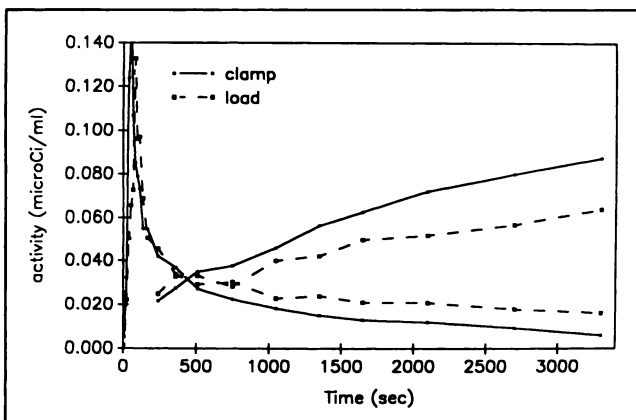


**FIGURE 5.** The myocardial and plasma time-radioactivity curves during a PET study after glucose loading and during insulin clamp (Patient 6, same representative images as in Figs. 3 and 4).

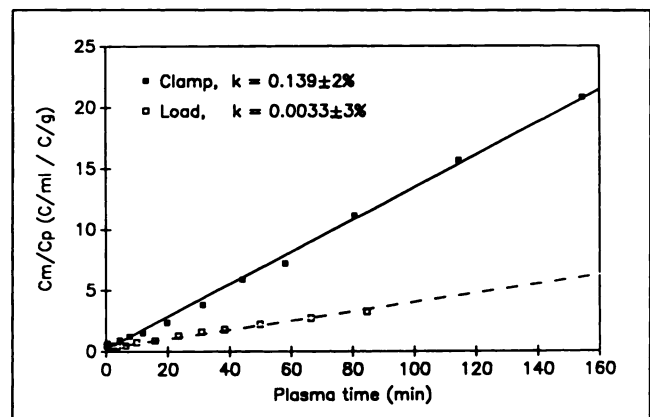


**FIGURE 6.** The graphical analysis of myocardial  $[^{18}\text{F}]\text{FDG}$  uptake after glucose loading and during insulin clamp (same ROIs as in Fig. 5).  $k$  = the slope of the plot  $\pm$  standard deviation.

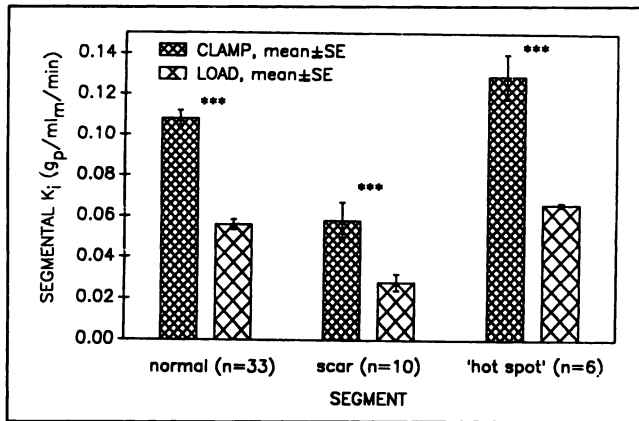


**FIGURE 7.** The mean segmental  $K_i$  values in normal and abnormal regions after glucose loading and during insulin clamp. \*\*\*  $p < 0.0001$  between load and clamp studies.

tients during both approaches (s.d. of rMGU was 26.3% after glucose loading and 22.5% during clamp). The intraindividual variation of rMGU in the normal segments was lower than the interindividual variation, but again there was no difference between the two approaches (s.d. of rMGU was 9.3% after glucose loading and 9.8% during clamp). In the septal segments, the rMGU was slightly lower (average 86%) and in the lateral and inferoposterior segments higher (average 112%) than the mean rMGU.

## DISCUSSION

Our experience with the insulin clamp technique as applied to PET studies shows that it is feasible to measure rMGU by [ $^{18}$ F]FDG and PET under adjustable steady-state conditions. The most widely used method to stimulate rMGU is glucose loading, which results in variable and unstable metabolic conditions. By definition, the Patlak approach for quantitative analysis requires steady-

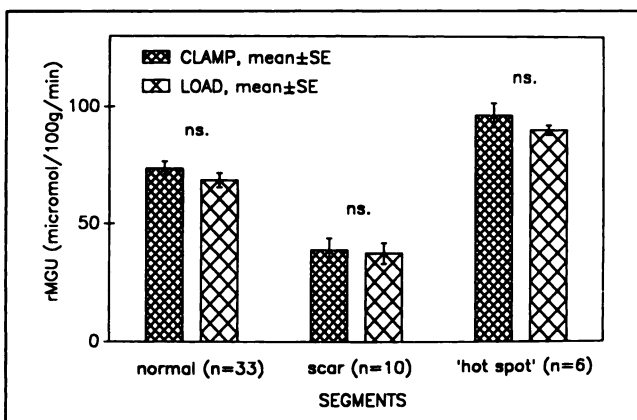


**FIGURE 8.** The mean segmental rMGU in normal and abnormal regions after glucose loading and during insulin clamp. ns = not significant difference between load and clamp studies.

state conditions (8). Therefore, the changes induced by glucose loading can introduce an error in rMGU calculations. In our study, the plasma-glucose levels were relatively high in three of the eight patients after 50 g glucose loading, which may indicate impaired glucose tolerance (11). There was no previous evidence of abnormal glucose metabolism in these subjects. However, patients with coronary artery disease have an increased prevalence for impaired glucose tolerance (31).

Krivokapich et al. (26) have shown that high plasma-glucose levels are associated with a lower fractional FDG utilization. This is concordant with the preliminary findings by Lee et al. (15) and Hicks (16) et al. that plasma-glucose levels bear an inverse relationship to the myocardium-to-blood-pool radioactivity ratio and image quality. This explains the lower measured  $K_i$  values after glucose loading compared to insulin clamp in our study, because the plasma-glucose levels were higher after glucose loading. In addition, the clearance of [ $^{18}$ F]FDG from the blood pool was enhanced during clamp, which also results in a higher myocardium-to-blood-pool radioactivity ratio and better image quality.

There was no difference in the calculated absolute rMGU values in the normal myocardial regions between the two approaches. We used a carefully determined, time-weighted mean plasma-glucose value during emission imaging for rMGU calculations after glucose loading. Thus, calculated rMGU values were comparable to those obtained during steady-state conditions, at least with the insulin and glucose levels used in our clamp. Also, in the report of Hicks et al. (16), rMGU values were found to be in the same range after glucose loading and during clamp.

The rate of [ $^{18}$ F]FDG utilization in myocardial scar regions during insulin clamp has not been reported previously. The rMGUs in the scar regions were reduced by an average of 46% compared with the normal myocardium in each patient and there was no difference in the absolute values obtained with the two approaches. Correspondingly, the observed increase of rMGU in some regions associated with critical coronary stenoses was comparable with both approaches.

It has been suggested that the insulin clamp technique can be used to standardize [ $^{18}$ F]FDG uptake in PET studies of the heart (17). However, we observed a similar degree of variability of the rMGU in normal myocardial segments within and between patients during both approaches. This can be explained by the fact that substrate availability is only one of the several factors that regulate myocardial glucose metabolism (9). However, the insulin clamp technique can be used to standardize substrate availability in studies primarily addressing the role of other factors affecting myocardial metabolism.

For rMGU calculations, we assumed that the LC remained unchanged during clamp and after glucose loading. However, there are no data for the LC during insulin clamp. In a recent study by Ng et al. (32), the LC was

found to respond to extreme changes of insulin and glucose concentrations in an isolated rabbit heart preparation when glucose was the only substrate for energy production. Previous studies performed during more physiological conditions have shown that the nutritional state does not affect the LC (26,33). In our study, the differences in plasma-glucose and insulin levels after glucose loading and during clamp were only moderate and, in addition, no hypoglycemia was caused. Also, there were no significant differences in the double products between the two protocols. Therefore, it is assumed that the LC is similar during euglycemic insulin clamp and after glucose loading.

The insulin clamp technique, although technically more demanding, has clear advantages over studies performed after glucose loading. It gives an adjustable metabolic steady state without altering the [<sup>18</sup>F]FDG uptake patterns in normal and abnormal myocardial regions. In addition, the image quality is excellent during clamp in patients with impaired glucose tolerance. The enhancement of [<sup>18</sup>F]FDG uptake by insulin clamp is so marked that it is possible to reduce the injected dose of [<sup>18</sup>F]FDG or perhaps shorten the imaging time and still obtain interpretable myocardial images. We have found that good quality images are obtained also with doses as small as 3–4 mCi of [<sup>18</sup>F]FDG during clamp. Since uninterpretable images after glucose loading are especially common in diabetic patients (16,34,35), the application of insulin clamp could be particularly helpful in enhancing myocardial [<sup>18</sup>F]FDG image quality in these patients. Our preliminary experience of insulin clamp in diabetic patients supports this (36,37). We currently use the insulin clamp in [<sup>18</sup>F]FDG studies performed for research purposes, especially when quantitation of rMGU is necessary, but also in clinical studies in patients with suspected or known impaired glucose tolerance.

## ACKNOWLEDGMENTS

The authors thank the technicians of The Turku Cyclotron-PET Center, especially Anne Helminen, Tarja Keskitalo, Leila Mäkinen, Ritva Heikola, Raija Nakolinna, Riitta Koskinen and Riitta Fabritius, for their skill and dedication throughout this study. We also express our gratitude to Dr. Kerttu Irjala for blood analysis and Prof. Veikko Koivisto and Dr. Hannele Yki-Järvinen for their help in planning the clamp protocol. This study was supported by a grant from the Turku University Foundation and the Jenny and Antti Wihuri Foundation.

## REFERENCES

- Fudo T, Kambara H, Hashimoto T, et al. F-18 deoxyglucose and stress N-13 ammonia positron emission tomography in anterior wall healed myocardial infarction. *Am J Cardiol* 1988;60:1191–1197.
- Brunken RC, Kottou S, Nienander CA, et al. PET detection of viable tissue in myocardial segments with persistent defects at Tl-201 SPECT. *Radiology* 1989;172:65–73.
- Berry JJ, Schwaiger M. Metabolic imaging with positron emission tomography. *Current Opinion in Cardiology* 1990;5:803–812.
- Marshall RC, Tillisch JH, Phelps ME, et al. Identification and differentiation of resting myocardial ischemia and infarction in man with positron computed tomography, F-18-labeled fluorodeoxyglucose and N-13 ammonia. *Circulation* 1983;67:766–788.
- Gambhir SS, Schwaiger M, Huang S-C, et al. A simple noninvasive quantification method for measuring myocardial glucose utilization in humans employing positron emission tomography and <sup>18</sup>F-deoxyglucose. *J Nucl Med* 1989;30:359–366.
- Sokoloff L, Reivich M, Kennedy C, et al. The <sup>14</sup>C-deoxyglucose method for the measurement of local cerebral glucose utilization: theory, procedure, and normal values in the conscious and anesthetized albino rats. *J Neurochem* 1977;28:897–916.
- Phelps ME, Huang SC, Hoffman EJ, Selin C, Sokoloff L, Kuhl DE. Tomographic measurement of local cerebral glucose metabolic rate in humans with (F-18)2-fluoro-2-deoxy-D-glucose: validation of method. *Ann Neurol* 1979;6:371–788.
- Patlak CS, Blasberg RG. Graphical evaluation of blood-to-brain transfer constants from multiple-time uptake data. Generalizations. *J Cereb Blood Flow Metab* 1985;5:584–590.
- Camici P, Ferranini E, Opie LH. Myocardial metabolism in ischemic heart disease: basic principles and application to imaging by positron emission tomography. *Prog Cardiovasc Dis* 1989;32:217–238.
- Gropler RJ, Siegel BA, Lee KJ, et al. Nonuniformity in myocardial accumulation of fluorine-18-fluorodeoxyglucose in normal fasted humans. *J Nucl Med* 1990;31:1749–1756.
- Nelson RL. Oral glucose tolerance test: Indications and limitations. *Mayo Clin Proc* 1988;63:263–269.
- DeFronzo RA, Tobin JD, Andres R. Glucose clamp technique: a method for quantifying insulin secretion and resistance. *Am J Physiol* 1979;237:E214–E223.
- Nuutila P, Knuuti J, Ruotsalainen U, et al. Glucose uptake in myocardial and skeletal muscle with positron emission tomography in type 2 diabetes [Abstract]. *Diabetology* 1990;33:A23.
- Hicks RJ, Herman WH, Kalff V, Wolfe E, Kuhl DE, Schweiger M. Effect of insulin and free-fatty acid levels on myocardial glucose metabolism demonstrated by PET-derived FDG kinetics [Abstract]. *J Nucl Med* 1990;31:398.
- Lee KS, vom Dahl J, Hicks RJ, Schweiger M. Relationship between glucose levels and F-18 fluoro-deoxyglucose image quality in cardiac PET studies [Abstract]. *J Am Coll Cardiol* 1991;17:120A.
- Hicks RJ, vom Dahl J, Lee KS, Herman WH, Kalff V, Schwaiger M. Insulin-glucose clamp for standardization of metabolic conditions during F-18 fluoro-deoxyglucose PET imaging [Abstract]. *J Am Coll Cardiol* 1991;17:381A.
- Hicks RJ, Herman WH, Halff V, et al. Quantitative evaluation of regional substrate metabolism in the human heart by positron emission tomography. *J Am Coll Cardiol* 1991;18:101–111.
- Hamacher K, Coenen HH, Stöcklin G. Efficient stereospecific synthesis of no-carrier-added 2-[<sup>18</sup>F]-fluoro-2-deoxy-D-glucose using aminopolyether supported nucleophilic substitution. *J Nucl Med* 1986;27:235–238.
- Solin O, Bergman J, Haaparanta M, Reissell A. Production of <sup>18</sup>F from water targets specific radioactivity and anionic contaminants. *Radiat Isot* 1988;39:1065–1071.
- Bergman J, Aho K, Haaparanta M, Reissell A, Solin O. Production of <sup>18</sup>F from H<sub>2</sub>O: specific radioactivity and chemical reactivity. *J Lab Comp Radiopharm* 1989;26:143–145.
- Henze E, Huang SC, Ratib O, Hoffman E, Phelps ME, Schelbert HR. Measurements of regional tissue and blood-pool radiotracer concentrations from serial tomographic images of the heart. *J Nucl Med* 1983;24:987–996.
- Hoffman EJ, Huang S-C, Phelps ME. Quantitation in positron emission tomography: 1. Effect of object size. *J Comput Assist Tomogr* 1979;3:299–308.
- Brunken RC, Schwaiger M, Grover-McKay M, Phelps ME, Tillisch J, Schelbert HR. Positron emission tomography detects metabolic activity in myocardial segments with persistent thallium perfusion defects. *J Am Coll Cardiol* 1987;10:557–567.
- Ratib O, Phelps ME, Huang S-C, Henze E, Selin CE, Schelbert HR. Positron tomography with deoxyglucose for estimating local myocardial glucose metabolism. *J Nucl Med* 1982;23:577–586.
- Krivokapich J, Huang SC, Phelps ME, et al. Estimation of rabbit myocardial metabolic rate for glucose using fluorodeoxyglucose. *Am J Physiol* 1982;243:H884–H895.
- Krivokapich J, Huang SC, Selin CE, Phelps ME. Fluorodeoxyglucose rate constants, lumped constant, and glucose metabolic rate in rabbit heart. *Am J Physiol* 1987;252:H777–H787.

27. Schiller NB, Shah PM, Crawford M, et al. Recommendations for quantitation of the left ventricle by two-dimensional echocardiography. *J Am Soc Echo* 1989;2:358-367.
28. Kadish AH, Little RL, Sternberg JC. A new and rapid method for the determination of glucose by measurement of rate of oxygen consumption. *Clin Chem* 1968;14:116-131.
29. Kuzuya H, Blix BM, Horwitz DL, Steiner DF, Rubenstein A. Determination of free and total insulin and C-peptide in insulin-treated diabetics. *Diabetes* 1977;26:22-29.
30. Camici P, Araujo L, Spinks T, et al. Increased uptake of 18-F-fluorodeoxyglucose in postischemic myocardium of patients with exercise induced angina. *Circulation* 1986;74:81-88.
31. Black HR. The coronary artery disease paradox: the role of hyperinsulinemia and insulin resistance and implications for therapy. *J Cardiovasc Pharmacol* 1990;15(suppl 5):S26-S38.
32. Ng CK, Holden JE, DeGrado TR, Raffel DM, Kornguth ML, Gatley SJ. Sensitivity of myocardial deoxyglucose lumped constant to glucose and insulin. *Am J Physiol* 1991;260:H593-H603.
33. Schneider CA, Rowe RW, Tewson TJ, Wong W-H, Taegtmeier H. Validation of 18-F-2-deoxy-2-fluoro-D-glucose as marker of myocardial glucose metabolism after brief periods of ischemia [Abstract]. *J Am Coll Cardiol* 1991;17:380A.
34. Lee KS, von Dahl J, Hicks RJ, Schweiger M. Relationship between blood glucose levels and 18-FDG fluoro-deoxyglucose image quality in cardiac PET FDG studies [Abstract]. *J Am Coll Cardiol* 1991;17:120A.
35. Bonow RO, Berman DS, Gibbons RJ, et al. Cardiac positron emission tomography. A report for health professionals from the committee on advanced cardiac imaging and technology of the council on clinical cardiology, American Heart Association. *Circulation* 1991;84:447-454.
36. Nuutila P, Knuuti J, Ruotsalainen U, et al. Glucose uptake in myocardial and femoral muscle in type 1 diabetes as determined with PET [Abstract]. *Diabetology* 1991;34:A58.
37. Nuutila P, Knuuti J, Ruotsalainen U, Teräs M, Wegelius U, Voipio-Pulkki L-M. Glucose utilization in myocardial and skeletal muscle in NIDDM estimated with <sup>18</sup>F-FDG using positron emission tomography (PET) [Abstract]. *Diabetes* 1990;39(suppl 1):86A.